Proceedings of the IASS 2024 Symposium
Redefining the Art of Structural Design
August 26-30, 2024, Zurich, Switzerland
Philippe Block, Giulia Boller, Catherine DeWolf,
Jacqueline Pauli, Walter Kaufmann (eds.)

Coupled Miura-ori Structure Along Space Curves

Sora MORIYAMA[a,c], Kuo-chih CHUANG[b*], Tomohiro TACHI[a*]

[a,*] The University of Tokyo
Tokyo, 153-8902
Tachi@idea.c.u-tokyo.ac.jp

[b,*] Zhejiang University
China, 310027
chuangkc@zju.edu.cn

[c] KAJIMA CORPORATION

Abstract

In the field of engineering and architecture, the programmability and universality of origami have received increasing attention. Origami techniques capable of approximating various shapes, including curved surfaces, are being explored. Such origami requires using sufficiently large sheets of materials relative to the target model, so it is challenging to scale this technique to an architectural scale. Since the industry provides the largest sheet materials in the roll form, the entire pattern consisting of rectangles is desirable from the point of material efficiency. Currently, the method for folding curves from a rectangular sheet is limited to planar curves; existing methods can obtain planar curves based on the Miura-ori pattern, while methods for obtaining space curves require sheets with curved boundaries. We recently developed the generalization of Miura-ori folding of rectangular sheets of paper into space curves. In this paper, we adopt this space curve folding technique to stiff and lightweight load-bearing structures. For this purpose, we propose to couple two extruded Miura-ori patterns to form a closed-cell sandwich structure. We show a method for obtaining such structures from given space curves. By solving the geometric compatibility between two sheets, we can realize the whole structure from a double-layered rectangular sheet. As a demonstrator, we build the stiff curved arch structure along a space curve by folding rolled sheet materials.

Keywords: origami, Miura-ori, morphology, curvature programming, paper material space structure

1. Introduction

In the field of architecture, efficient methods for generating curved elements from linear members are required to achieve a variety of forms chosen for aesthetic and structural reasons. Several techniques have been proposed. Traditional bentwood or plastic forming of steel members can achieve desired curves but requires prescribed molds or formworks. Also, the forming process limits the resulting shapes to planar curves. Recently, actively bending and deforming linear materials such as wood or elastic elements have been investigated [1, 2]. These methods do not require molds; however, they are limited in their shapes, namely to elastica curves. CNC-based methods of creating prescribed space curves with wood have also been proposed [3, 4]. In these studies, a CNC was used to carve wood and produce wooden structures along the target space curve.

We study origami as a method for efficiently producing prescribed curved elements by folding linear sheet materials often provided in the roll form. Currently, the method for folding curves from strip-shaped sheet materials is limited to planar curves [5, 6]. On the other hand, methods for obtaining space

curves require sheets with curved boudnary [7], which is significantly inefficient to be cut out from a strip and cannot be applied to our objective. We recently developed the generalization of Miura-ori folding of rectangular sheets of paper into space curves [8]. This method allows for the control of the two directional curvatures: the normal curvature and the geodesic curvature.

However, simply applying this method to large-scale structures had a structural problem. Although the pattern has a cross-section that resembles an I-beam achieved by the insertion of a center strip, there is a challenge of local buckling due to a high width-to-thickness ratio when thin material is used. In this paper, we address this structural problem by coupling two beam-like origami into a closed cross-section. To make this work, the two beam-like structures need to be compatible when they are folded and unfolded. We extend the origami curved beam design method [8] and generate a pair of compatible origami structures with slightly different crease patterns from the prescribed target curves. This model, in its folded state, constructs a closed-cell structure along the target space curve, preventing flange buckling.

Section 2. overviews the authors' work [8] describing a design method for Miura-ori along a single space curve. Section 3. addresses the structural issues when the structure is scaled up and provides the key concept of coupling. Section 4. shows the compatibility between the two patterns and proposes a design method to construct a coupled Miura-ori structure along the target space curve. Section 5. overviews the fabrication method for a pavilion using this technique.

2. Programming two-directional curvatures

This section overviews the technique for providing two-directional curvatures by folding Miura-ori provided by the authors [8].

2.1. Definition

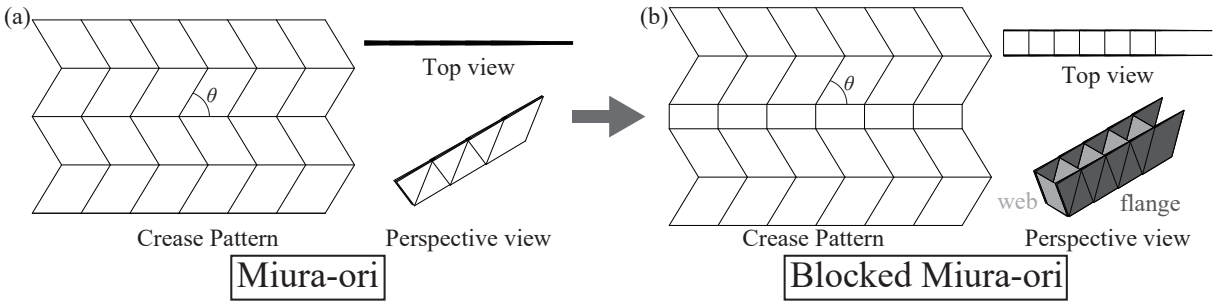

Figure 1: Notations for Miura-ori and blocked Miura-ori. The sector angle θ is the angle between adjacent segments on the panel. This blocked Miura-ori is the basis of our method.

Miura-ori, a pattern with congruent parallelograms, can be flat-folded into a thin plate according to Kawasaki theorem (see left in Figure 1). This study starts with the shape produced by the flat-folded state of the Miura-ori and varies their patterns to form curvature. However, the flat-folded state cannot be a stable structural element by itself because it acts as a thin plate and can easily bend under external forces. To increase the inertia of the moment of the section, a *center strip*, i.e., a series of rectangular panels, is inserted in the crease pattern. This portion of the pattern cannot fold flat when the rest of the pattern is folded flat, creating a block state that has a three-dimensional shape while maintaining structural rigidity, this state is referred to as a completely folded state. This blocking technique is being researched as a structural application of Miura-ori, such as the core of sandwich panels [9]. We call the model with the extrusion a *Miura-ori beam*, and it is expected to resist external forces like the shapes

commonly used in architecture, such as I-beams. We call the completely folded sections that originally made up the Miura-ori *flange* and the center strip folded in a zigzag the *web*.

2.2. Pattern-Curvature relation

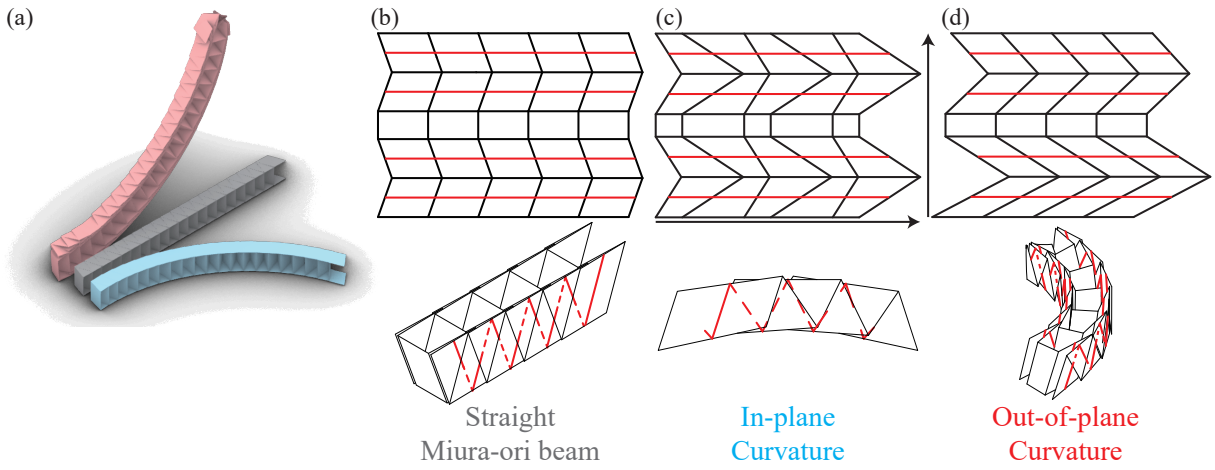

Figure 2: Three types of crease patterns form different curvatures (a). A pattern with identical sector angles forms the straight Miura-ori beam (b). A pattern with the sector angles varying along the strip direction forms the Miura-ori beam with in-plane curvature (c). A pattern with the sector angles varying in transverse direction forms the Miura-ori beam with out-of-plane curvature (d).

In the crease pattern, the angle formed by the parallel lines and the diagonals is called the *sector angle* θ. In the original Miura-ori beam, all sector angles are identical except for the center strip. When these sector angles are appropriately varied, we obtain two types of curvature. Assuming that the flange is the base plane to define the orientation, we call *in-plane* and *out-of-plane* curvature when they are curved within the plane and curved out of the plane, respectively.

To annotate the angle variations, we provide the following model. We call the groups of panels separated by lines parallel to the strip direction *rows*. Each row is denoted by index j. The polyline connecting the midpoints of the consecutive creases in each row is called the *center line*. When the pattern is completely folded, this center line forms a *zigzag line*.

The zigzag line characterizes the folded shape of each row, so we can inversely model the folded state by specifying the zigzags. The half of the exterior angles of the zigzag line correspond to the sector angle of the Miura-ori. Thus, when the zigzag line can be drawn along the curves, the pattern of Miura-ori can be calculated from it.

When we consider the distance between alternating vertices of zigzags, they become shorter when the corresponding sector angle is closer to 90° and longer when the sector angle is smaller. Therefore, alternating large and small sector angles along the strip direction results in the zigzag lines curved along the flange plane, producing *in-plane* curvature. On the other hand, grading sector angles perpendicular to the strip direction results in different effective lengths of flat-folded rows between folded layers, thus producing the *out-of-plane* curvature.

2.3. Realizing curves on surfaces

When the two curvatures are controlled simultaneously, a structure along a space curve is obtained. The shape of the proposed curved structure can be specified by a space curve and an orientation that defines

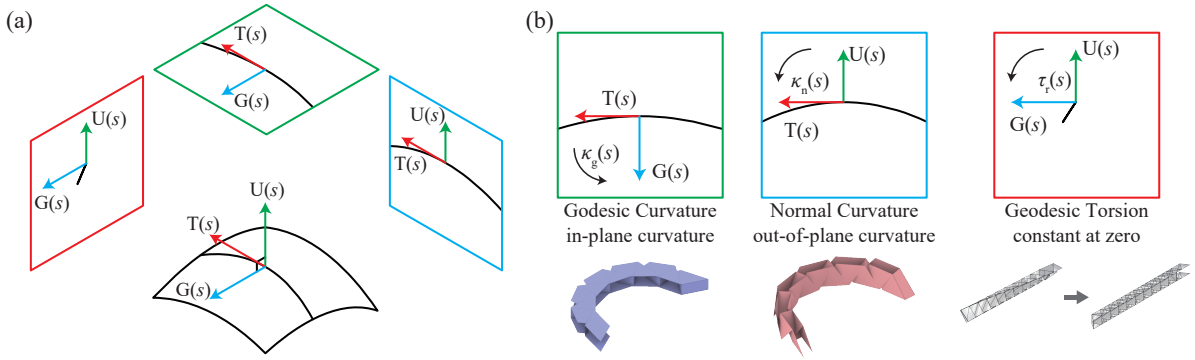

Figure 3: Curvatures of a curve on a surface and their relation to the folded shapes. Geodesic curvature, normal curvature, and geodesic torsion defined by the Darboux frame of the target curve correspond to the in-plane curvature, out-of-plane curvature, and elastic torsion of the Miura-ori beam.

the in-plane and out-of-plane directions. We model the curve with orientation using the Darboux frame, which is constructed on a curve that lies on a surface. Here, we set the normal direction of the flange to be the normal of the surface. The Darboux frame is composed of three orthogonal vectors: the tangent vector $\mathbf{T}(s)$, the surface normal vector $\mathbf{U}(s)$, and the tangent normal vector $\mathbf{G}(s)$ (see Figure 3).

$$d\begin{pmatrix}\mathbf{T}\\ \mathbf{G}\\ \mathbf{U}\end{pmatrix} = \begin{pmatrix}0 & \kappa_g ds & \kappa_n ds\\ -\kappa_g ds & 0 & \tau_g ds\\ -\kappa_n ds & -\tau_g ds & 0\end{pmatrix}\begin{pmatrix}\mathbf{T}\\ \mathbf{G}\\ \mathbf{U}\end{pmatrix}. \tag{1}$$

In Darboux frame, three independent functions of arclength s control a curve on a surface: geodesic curvature $\kappa_g(s)$, normal curvature $\kappa_n(s)$, and geodesic torsion $\tau_g(s)$. The in-plane and out-of-plane curvatures are represented by the geodesic curvature κ_g and the normal curvature κ_n, respectively. Thus, properly controlling the sector angles in horizontal and vertical directions can control these curvatures. On the other hand, the geodesic torsion $\tau_g(s)$ is determined by the elastic deformation of the entire beam; specifically, the obtained curve is expected to have $\tau_g(s) = 0$ under no external load since the flange and the web of the structure rest in a zero-torsion state. When approximating a space curve, the target curve is restricted to the curves with zero geodesic torsion $\tau_g = 0$, which is known to be equivalent to a principal curvature line of the surface [10]. We chose the principal curvature lines of an ellipsoid as a demonstrating example of a space curve with two directional curvatures (see Figure 4).

2.4. Computing Prescribed Curves

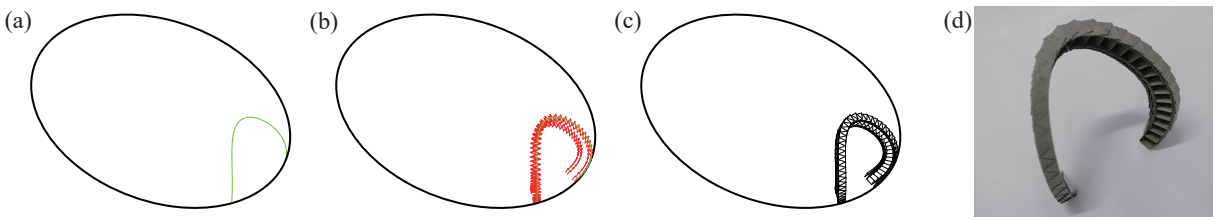

Figure 4: The flow of geometric construction of curved beam. To obtain the curved Miura-ori beam, the target surface and curve are defined, the layers of zigzag lines are drawn along the target curve, the zigzag lines are optimized to satisfy constraints, and then, the crease pattern is calculated.

The Miura-ori pattern is designed by using the principal curvature line as the target curve and creating a zigzag line to this curve. First, the target surface and the principal curvature line are determined. A zigzag line is drawn on the target surface along the curve and then repeated by the number of rows in the normal direction of the surface to make the zigzag lines. The zigzags for different layers need to have correct edge lengths and positions, for which we use an optimization scheme described below. From the generated zigzag lines, the sector angle θ and the segment length can be determined, allowing the creation of a crease pattern. By folding the pattern, we could get the model approximating the target curve.

2.5. Constraint for creating the zigzag lines

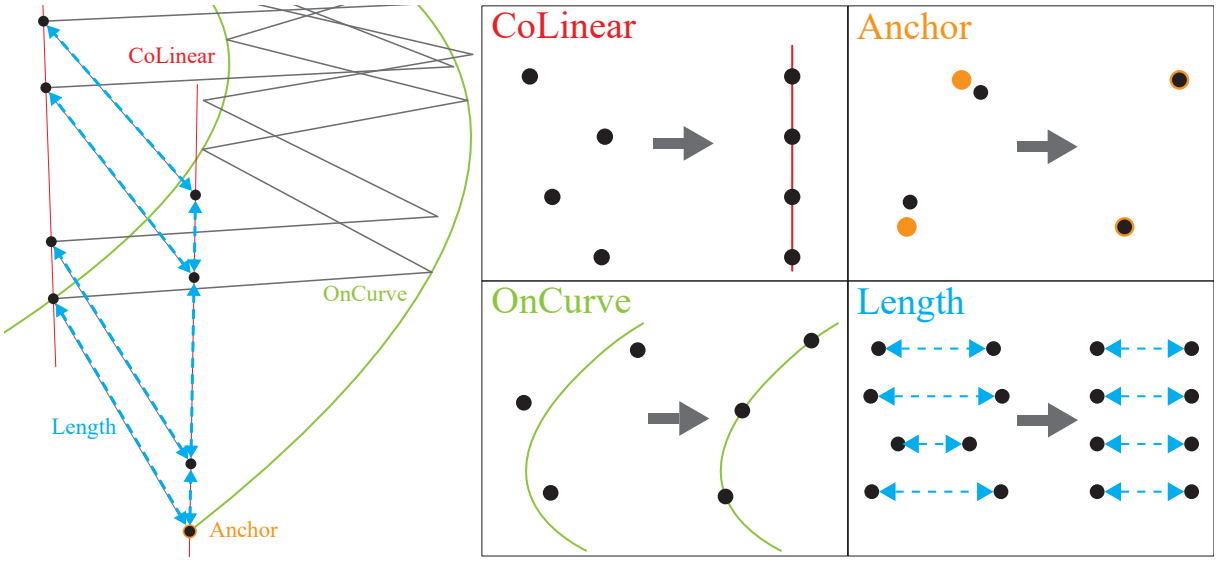

Figure 5: Constraint between layers of zigzags. To obtain the proper zigzag lines to calculate the Miura-ori beam pattern, "Length," "CoLinear," "Anchor," and "OnCurve" of Rhinoceros/Grasshopper Kangaroo2 [11] are used as the functions.

The thickness $t_{j,j+1}$ between adjacent layers of zigzags is determined by the thickness of sheet material t and the extrusion H. In a completely folded Miura-ori, without extrusion, the ideal thickness is $t_{j,j+1} = 4t$. The thickness between zigzags separated by center stirp is $t_{j,j+1} = 4t + H$. For the crease pattern to be compatible between rows, the segment lengths need to be equal between layers. In particular, we make all the segment lengths of the zigzag lines to a prescribed length.

To make these geometric constraints realized, we use a relaxation-based optimization scheme implemented in Kangaroo2 [11] system of Rhinoceros/Grasshopper. We use Goal Objects "Length," "CoLinear," "Anchor," and "OnCurve" to implement the constraints. These help ensure segment length uniformity, position zigzags on top of each other, and fix the zigzags in the correct positions. The optimization function prioritizes segment length uniformity by giving the Length constraint a significant weight while keeping other constraints weakly weighted to be used for regularization.

3. Structural performance of Miura-ori beams

A unique feature of the curved Miura-ori beam is the possibility of creating space-curved models from rectangular sheet materials. Especially in industry, the largest sheet materials are provided by roll forming. As the demonstrator, we aim to construct a meter-scale pavilion, specifically an arch structure

along a target space curve with a height of about $2.6\,\mathrm{m}$, by applying the method to the roll sheet of paper or plastics with approximately $1\,\mathrm{m}$ in width and $25\,\mathrm{m}$ in length. We first fabricated the structure with a single sheet and identified the buckling problem when the thin sheet was used (3.2.). To prevent the buckling, we then propose structures composed of two sheets of materials, forming a closed-cell structure (3.3.).

3.1. Single-sheet small model

For the initial test, a $1:10$ scale model was created using a sheet of paper with a thickness of approximately $0.1\,\mathrm{mm}$ (Tant $100\,\mathrm{kg}$, equivalently $\sim 116\mathrm{g/m}^2$, Takeo Co. Ltd.). The dimensions of the model are about $260\,\mathrm{mm}$ in height and $210\,\mathrm{mm}$ in width. The arch section had a rectangular cross-section of $10\,\mathrm{mm}$ by $20\,\mathrm{mm}$. The thickness-to-wavelength ratio that determines the buckling behavior is $1:140$. The pattern was perforated using a CNC cutting plotter and folded manually. To fix the structure in the target position, it is necessary to bind the completely folded sheets at the flange. For this scale model, a wet fixation using glue was adopted. With this scale of model, the construction of the arch was successfully achieved (see left in Figure 6).

With this model, we applied a concentrated loading of $10\,\mathrm{N}$, which is more than 30 times its self-weight. Therefore, we expect the structure to be scaled up by 10 times following the Square-Cube law (self-weight being 1000 times while the cross-section being 100 times). In addition, if we expect the structure to support its load by the tension and compression (membrane force) along the sheet, the thickness of the sheet does not matter as if thickness increases by x times, the self-weight increases by x times. This assumption turns out to be incorrect, as later described.

3.2. Single-sheet large model

Following the above discussion, we first tried to scale up the model by 10 times in length and width, while increasing the thickness by 2.5 times. Specifically, the model was created using craft paper (insulation paper or pressboard) with a thickness of approximately $0.25\,\mathrm{mm}$. This makes the thickness-to-wavelength ratio $1:560$. Using a CNC roll-cutting plotter, crease patterns were perforated on roll sheet material with $880\,\mathrm{mm}$ in width and $24\,140\,\mathrm{mm}$ in length. Then, the pattern was manually folded to create an arch structure model with a width of $2100\,\mathrm{mm}$ and a height of $2613\,\mathrm{mm}$. The cross-section had a rectangular shape measuring $100\,\mathrm{mm}$ by $200\,\mathrm{mm}$. Considering the need for disassembly, transportation, storage, and reuse after the exhibition, a dry fixation method was used to bind the flange. Cable ties are used for dry fixation.

The model did not hold its self-weight due to buckling in the flanges caused by its weight. Despite the dimensions being scaled up by a factor of ten, the thickness increased only by about 2.5 times, leading to a smaller thickness-to-wavelength ratio and making the structure more susceptible to buckling under its weight (see Figure 6). There are possible solutions to avoid these buckling. (1) Using thicker materials to reduce the width-to-thickness ratio is a straightforward solution to accommodate scaling up; however, we are interested in exploring solutions within the origami techniques that can address this issue without necessarily relying on material thickness. (2) Another solution for preventing buckling is to use wet fixation to make the multi-layered sheets on the flange act as composite beams instead of dry fixation that made the layers superpositioned beams. However, this will lose the advantage of repeatedly folded and unfolded. (3) Therefore, we show an alternative method to enhance stability and resistance to buckling in large-scale structures based on the coupling of folded sheets. This method leverages the inherent geometric and structural advantages of origami, as it can be made with thin sheets and be repeatedly folded and unfolded.

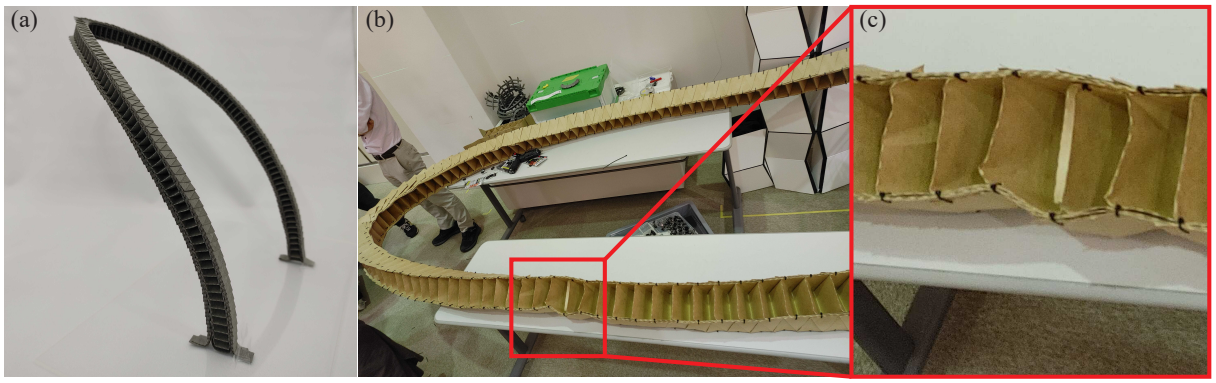

Figure 6: Small and large single-sheet models. The left figure shows the 1:10 scale model, the center shows the 1:1 scale model and the right shows the buckling behavior when trying to construct the model.

3.3. Coupled sheet model

The cause of buckling in the Single-sheet Large Model happens at the open edge of the flange. This is because the open edge cannot counteract compressive forces. A previous study [9] uses Miura-ori as the core of the sandwich structure to solve the problem. We present a method based on coupling curved Miura-ori structures to eliminate these open edges and form a closed-cell structure. Combining two sheets to create a coupled Miura-ori is expected to improve the capacity against buckling.

4. Designing coupled Miura-ori beams

4.1. Coupling conditions

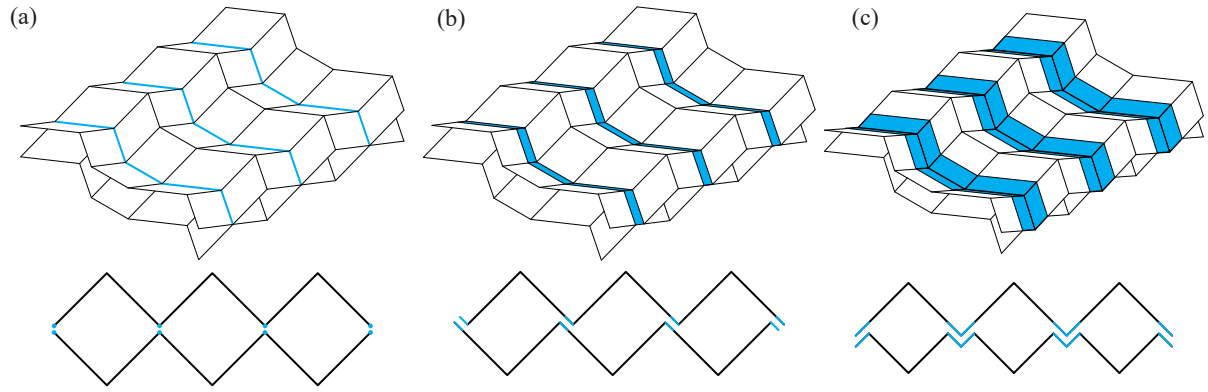

Figure 7: Different coupling methods of Miura-ori beams. The blue region shows the shared parts of two structures used for bonding. The top figures show coupled Miura-ori beams and the bottom figures show the corresponding zigzag lines.

To generate a pair of compatible Miura-ori beams, we consider generating the beams using a pair of zigzag lines. First, we consider the fixation method in the case where the beam is straight.

If the two zigzags share only at the vertices, the two sheets will form a line contact (see left in Figure 7). For construction, it is preferable that the two sheets can be bonded in such a way that surface contact is possible. To make the coupled structure a closed-cell structure with tubular profiles, we let the two zigzags partially share the edges for the adhesion regions.

The simplest zigzag lines with partial overlap are those that overlap each other with a slight sliding

to each other (middle in Figure 7). This coupling idea is equivalent to the rigidly foldable coupling of Miuira-ori [12]. Despite its simplicity, this parallel alignment is difficult to accurately align, as an arbitrary amount of sliding can happen when they are bonded together.

To improve the alignment accuracy, we propose an alternative pattern by inverting the tips of the vertices of zigzag lines to create the V-shaped adhesion region, which we call a *pocket* (see right in Figure 7). The vertex of one sheet self-aligns and interlocks at the pocket of the other sheet; they keep face contact after adhesion.

A single Miura-ori beam is developable. However, the coupled sheets are not necessarily developable. To make the coupled Miura-ori model compactly stored, transported, deployed, and stored again in rolls while keeping the two sheets combined, we need the developability of the structure even when two sheets are combined. For this developability, the closed quadrilaterals formed by two zigzags need to be parallelograms (with opposite segments of equal lengths). In the following method, we use the special case when these quadrilaterals form rhombuses, i.e., all segments are equal in length. Note that the structure is rigidly foldable if the beams are straight. However, if the structure has curvature, the pattern is no longer rigidly foldable.

4.2. Generating coupled structures from a space curve

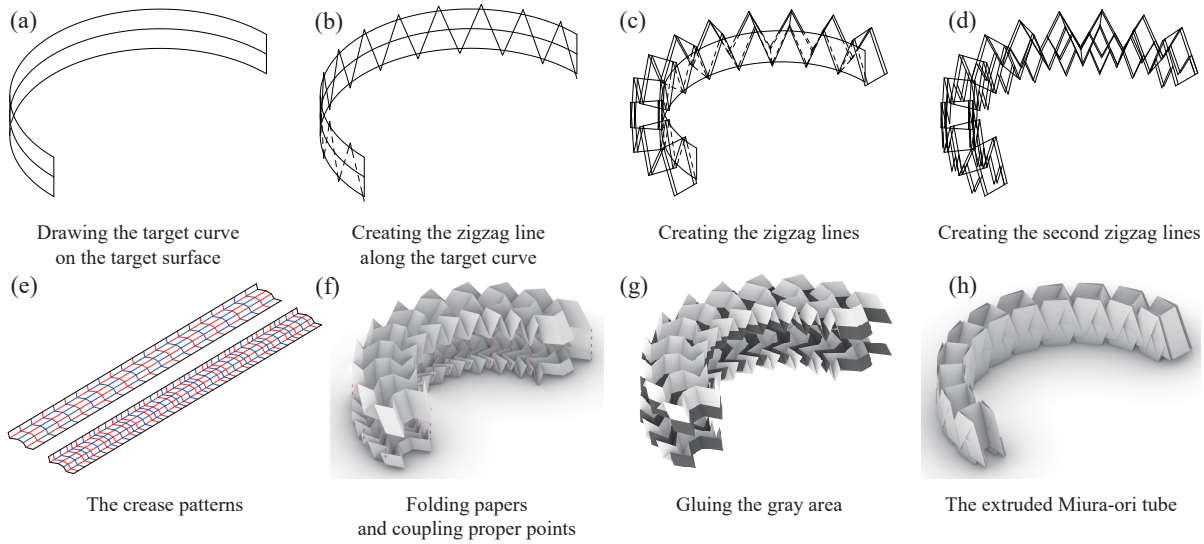

Figure 8: The flow of constructing the Miura-ori tube structure To construct the Miura-ori tube structure, the pattern can be calculated based on the method of programming two-directional curvature and the conditions for the coupled structure.

We simplify the calculation of a pair of zigzag lines by computing one zigzag line and derive the second zigzag line from the first. Coupled structures along the target space curves are created by following the following steps. First, as in Section 2., we create a target curve and the surface based on the principal curvature line.On this curve, a first set of multiple zigzag lines are drawn, and the lengths and positions are optimized. This set represents a single Miura-ori beam. From this first set of zigzag lines, the second set of zigzag lines are drawn to satisfy the conditions for creating a pocket and the rhombuses. Specifically, we take a V-shaped part of the zigzag at each vertex and invert it to the other side. The Miura-ori patterns on two sheets are calculated by measuring the exterior angle of the zigzags and using their haves as the sector angles of the panels. By folding and then fixing two sheets, we can construct a cellular structure along the target curve.

5. Demonstrator

5.1. Design for detail

To demonstrate the feasibility of our method, we propose the following design of an arch. As for the geometry, we use a portion of one of the principal curvature lines of the ellipsoid. Although we build a single curve, we consider that we can make a grid shell of the entire surface by drawing the grid of principal curvature lines.

We generate crease patterns by our proposed method for a roll sheet material of two PET materials of about width $0.7\,\mathrm{m}$ × length $23\,\mathrm{m}$. The thickness is $0.2\,\mathrm{mm}$ and the areal density is $400\,\mathrm{g/m^2}$. The arch model to be create is about width $2.6\,\mathrm{m}$ × height $2.7\,\mathrm{m}$.

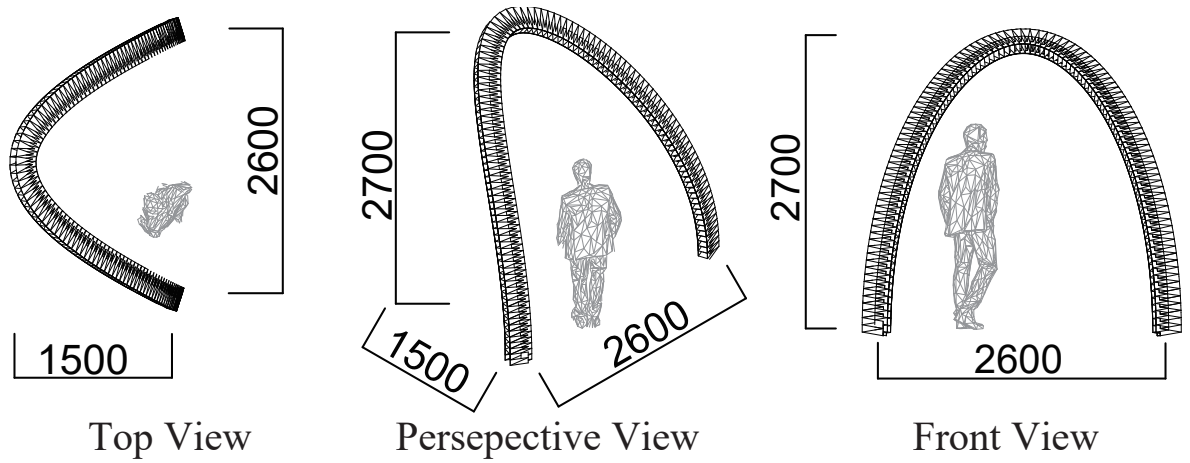

Figure 9: Demonstrator design of our method.

5.2. Structural details for the ends

When constructing the arch, it is necessary to design the end structures, *piers*, to be fixed on the ground. The piers are desirable to be in proper contact with the ground and to be close to vertical to the ground so that the load is efficiently conveyed to the ground. For this purpose, we extend the original space curve of the principal curvature lines vertically and use the continuous curve for the construction of Miura-ori beams so that the arch part and the pier structures are constructed continuously. We apply the proposed construction method for this extended curve. When creating the zigzag lines, each end of the zigzag line is modified to the lines on the ground plane so that the obtained web has face contact with the ground.

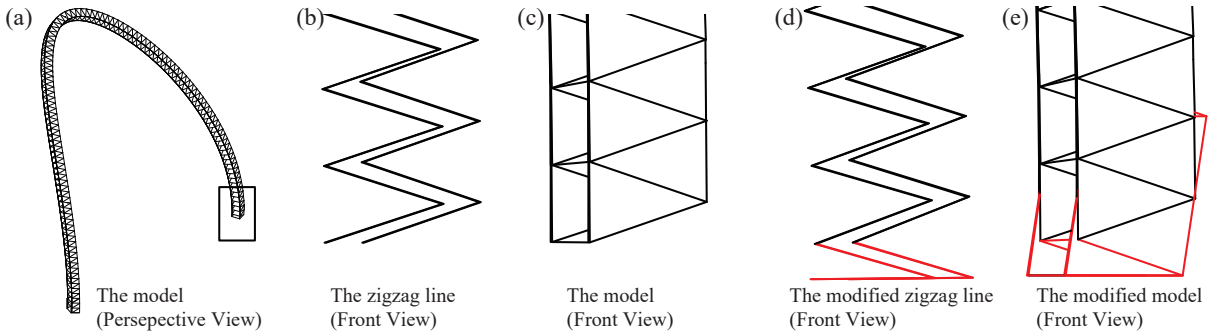

Figure 10: Detail of the end of the arch model. By modifying the zigzag lines, the end of the arch model was given a plane to face contact with the ground.

6. Outlook

We developed a method to fabricate a stiff yet lightweight structure along a space curve by coupling two curved Miura-ori beams. By combining two beam structures with open sections to form a closed-cell sandwich structure, we made a system that is less prone to buckling, even with an extremely low thickness-to-width ratio. Our geometric approach enables the creation of these structures from a pair of thin materials and can be formed into arbitrary curved shapes in space. The realization and physical experiments on the demonstrator are the future work of this study. This origami-inspired technique is versatile and applicable across scales from micro to architectural. However, it currently requires manual folding post-pattern printing. In the future, we would like to explore the automatic way of folding the proposed structures based on either self-folding or roll-to-roll robotic folding for broader industrial use.

References

[1] T.-U. Lee and Y. M. Xie, "From ruled surfaces to elastica-ruled surfaces: New possibilities for creating architectural forms," in *Proceedings of IASS Annual Symposia*, International Association for Shell and Spatial Structures (IASS), vol. 2020, 2020, pp. 1–12.

[2] E. Xie, T. Jiang, Z. Xia, and W. Xu, "Postbuckling behavior of frp bending-active arches subjected to a central point load," *Journal of Composites for Construction*, vol. 27, no. 5, p. 04 023 039, 2023.

[3] B. SATTERFIELD *et al.*, "Bending the line: Zippered wood creating non-orthogonal architectural assemblies using the most common linear building component (the 2x4)," in *Fabricate 2020: Making Resilient Architecture*. UCL Press, 2020, pp. 58–65, ISBN: 9781787358126. [Online]. Available: `http://www.jstor.org/stable/j.ctv13xpsvw.12` (visited on 12/24/2023).

[4] R. Naboni, A. Kunic, D. Marino, and H. Hajikarimian, "Robotic zip-bending of wood structures with programmable curvature," *Architecture, Structures and Construction*, vol. 2, no. 1, pp. 63–82, 2022.

[5] L. H. Dudte, E. Vouga, T. Tachi, and L. Mahadevan, "Programming curvature using origami tessellations," *Nature materials*, vol. 15, no. 5, pp. 583–588, 2016.

[6] Y. Klett and K. Drechsler, "Designing technical tessellations," in *Origami*, ISBN 1568817142, P. and Wang-Iverson, R. Lang, and M. Yim, Eds., vol. 5, CRC Press, 2011, pp. 305–322.

[7] T. Tachi, "One-dof rigid foldable structures from space curves," in *Proceedings of the IABSE-IASS Symposium*, 2011, pp. 20–23.

[8] S. Moriyama, K.-C. Chuang, and T. Tachi, "Folding a strip into space curves," in preparation.

[9] S. Fischer, S. Heimbs, S. Kilchert, M. Klaus, and C. Cluzel, "Sandwich structures with folded core: Manufacturing and mechanical behavior," in *International SAMPE Europe Conference, Paris*, 2009.

[10] E. Abbena, S. Salamon, and A. Gray, "Modern differential geometry of curves and surfaces with mathematica," in CRC Press, 2017, ch. CH.17.

[11] D. Piker, *Kangaroo 2*, `https://github.com/Dan-Piker/K2Goals`, 2015.

[12] Y. Klett and P. Middendorf, "Face to face: Varieties and properties of coplanarly joined multilayer tessellations," in *Proceedings of IASS Annual Symposia*, International Association for Shell and Spatial Structures (IASS), vol. 2016, 2016, pp. 1–7.